ChemComm

COMMUNICATION

Cite this: *Chem. Commun.*, 2019, **55**, 4797

Received 10th January 2019,
Accepted 26th March 2019

DOI: 10.1039/c9cc00248k

rsc.li/chemcomm

Structurally simple trimesic amides as highly selective anion channels†

Lin Yuan,‡[a] Jie Shen,‡[b] Ruijuan Ye,[c] Feng Chen[b] and Huaqiang Zeng *[b]

Trimesic amide molecules, which contain simple alkyl chains in their periphery, exhibit interesting anion-transport functions. The most active and highly selective channel TA12 efficiently transports ClO_4^- anions across membranes, with other anions conducted in the order of $I^- > NO_3^- > Br^- > Cl^-$.

Cellular ion homeostasis across membranes is precisely maintained by biological ion transporters, which mostly transport ions through a channel mechanism. Malfunctioned protein ion channels often result in dysregulated ion transport and could lead to various 'channelopathies' such as cystic fibrosis (Cl^-), iodide deficiency disorders, paralysis (Na^+), seizure (K^+) and malignant hyperthermia (Ca^{2+}). Synthetic ion channels have thus been actively pursued since 1982,[1] aiming not only to elucidate the possible ion transport mechanisms but also to promote medical applications in ''channel therapies''.[2]

Considering that protein ion channels often contain a narrow-sized cavity for ion transport, rationally designed synthetic ion channel molecules mostly carry either central macrocyclic units, tubular cavities, or one-dimensionally aligned ion-binding/transport units[2f,3] as ion permeation pathways.

On the other hand, some naturally occurring pore-forming peptides[4a–d] and their synthetic analogues[4e–i] readily assemble, *via* side chain–side chain interactions, into a barrel stave pore for mediating the killing of bacterial cells. Similar side chain–side chain interactions are also ubiquitously observed during the formation of α-helix bundles,[5a–e] protein channels,[5f,g] and pore-forming toxins[5h] from their constituent units. We believe that this type of side chain–side chain association mode, when used appropriately, might open a new avenue for designing novel types of synthetic transmembrane channels, greatly expanding both the structural and functional repertoires of synthetic channel systems.[6] Nevertheless, this strategy currently still remains largely unexplored.

Trimesic amides (**TA**s) are an interesting class of molecules that have been investigated quite intensively in crystal design and growth[7a,b] as well as materials science.[7c,d] In **TA**s, the three amide groups do not stay coplanar with the central benzene ring, but they are not perpendicular to the central ring either. This interplanar tilting angle of the amide groups with respect to the aromatic ring plane highly depends on the peripheral substituents.[7b] With the use of peripheral butylbenzene groups as in **TA4** (Fig. 1a), the amide groups, being perfectly self-complementary to each other in H-bond-forming character, generate a triple helical network of intermolecular H-bonds (Fig. 1b).[7b] This H-bonding network subsequently links **TA4** molecules into π-stacked discotic 1D rods in the solid state, with peripheral butylbenzene groups organized into a hexagonal arrangement. Further association among these 1D rods similarly proceeds in the form of hexagonal packing, creating numerous sizeable voids/channels of 2 Å across (Fig. 1c).

Although the enclosed channels found in $(\mathbf{TA4})_n$ are likely either too narrow for ion conduction or show low activity in ion transport, the existence of such channels is highly interesting and inspiring from which we could quickly envision a novel ion channel system. More specifically, we anticipated that a simple extension of *n*-butyl chains to longer alkyl chains from hexyl to tetradecyl chains (Fig. 1a) might result in the formation of a larger pore as schematically exemplified by $(\mathbf{TA12})_6$ (Fig. 2a). In the fortunate scenarios, these larger pores may enable ions to get transported across membranes, with ion transport activities further tunable *via* tuning length and type of the alkyl chains as well as other functional groups. We further anticipated that anions should be transported more easily than cations as the alkyl chains, which decorate the pore interior, should interact more favourably with hydrated anions than hydrated cations. Here, we confirm our hypotheses and show that **TA**s, when

[a] *College of Chemistry and Bioengineering, Hunan University of Science and Engineering, Yongzhou, Hunan, 425100, China*
[b] *Institute of Bioengineering and Nanotechnology, 31 Biopolis Way, The Nanos, 138669 Singapore. E-mail: hqzeng@ibn.a-star.edu.sg; Tel: +65-6824-7115*
[c] *Department of Chemical and Biomolecular Engineering, National University of Singapore, 117585 Singapore*

† Electronic supplementary information (ESI) available: Experimental procedures and ion transport activities. See DOI: 10.1039/c9cc00248k

‡ These authors contributed equally.

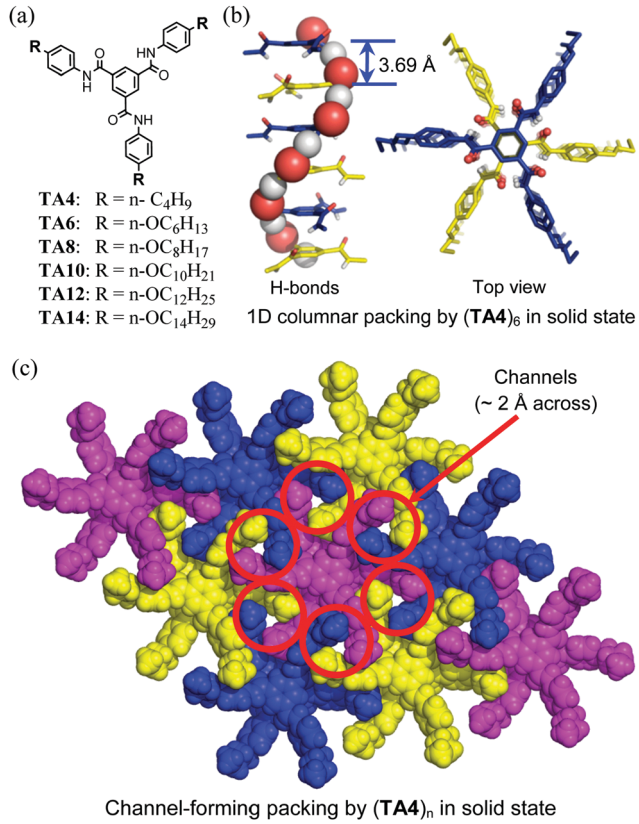

Fig. 1 (a) Structures of trimesic amide molecules studied in this work. (b) One-dimensional columnar packing of (**TR4**)$_6$ supported by a triple helical H-bonding pattern. (c) Two-dimensional arrangement of 1D rods that lead to the formation of sizable channels/voids of 2 Å across.

modified to carry longer alkyl chains, do can function as good anion-transport channels.

A well-established HPTS-based LUV assay (Fig. 2b) was then adopted for evaluating ion transport activities of five **TA** channels (**TA*n***, n = 6, 8, 10, 12 and 14). The principle behind this assay is that ion exchange, occurring in one of the four possible modes (Na^+/H^+ antiport, Na^+/OH^- symport, Cl^-/OH^- antiport or Cl^-/H^+ symport), will result in an increase in intravesicular pH, which in turn increases the fluorescence intensity of a pH-sensitive HPTS dye. Plotting changes in fluorescence intensity *vs.* time at the same channel concentration therefore allows one to compare the relative ion transport abilities of ion channels.

At 20 μM, **TA8** displays the highest fractional ion transport activity, which is followed by **TA10** > **TA6** > **TA12** > **TA14** (Fig. 2b). This trend in ion transport activity persists when the chloride-sensitive SPQ assay was carried out to evaluate the chloride-transport abilities of these channels (Fig. 2c). Furthermore, using the LUV assay involving 200 mM Na_2SO_4 (Fig. 2d), all **TA** channels at 20 μM produce smaller increases in fluorescence intensity than the background signal, indicating the influx of H_2SO_4 to some varying extent, rather than the influx of Na^+ ions, under a high ionic concentration gradient in the presence of **TA** channels. In sharp contrast, gramicidin A (gA) results in a fluorescence increase by 60% at an extremely low concentration of 1 nM (Fig. 2d) as a result of the rapid influx of Na^+ ions and efflux of H^+ ions. Similar results were obtained when 200 mM K_2SO_4 was used (Fig. 2d). These three sets of data shown in Fig. 2b–d unambiguously establish chloride anions as one of the main transport species. In other words, either the Cl^-/OH^- antiport or Cl^-/H^+ symport should account for the ion transport mediated by the five **TA** channels.

Valinomycin (**VA**), a potent K^+ carrier, was then introduced in the LUV-based assay to compare the transport rates between Cl^- and OH^- (Fig. 2e). To maintain charge neutrality, a **VA**-mediated influx of K^+ ions will be accompanied by the influx of either Cl^- or OH^- anions (or efflux of H^+ ions), which respectively cause either negligible or significant increases in fluorescence intensity. Experimentally, addition of **VA** at 3 pM leads to increases of 3.6% (*e.g.*, 31.5–37.9%) in the presence of **TA8** and of 2.9% (*e.g.*, 12.7–9.8%) in the absence of **TA8**. The relative change of 0.7% (*e.g.*, 3.6–2.9%) is obviously insignificant, thereby supporting the Cl^- transport rate to be much faster than that of OH^- or H^+ ions. This conclusion is also consistent with that drawn from FCCP-based assay (Fig. S1, ESI†).

Additionally, given the highly hydrophobic nature of the pore, hydrated OH^- anions should be transported more preferentially than hydrated H^+ ions. In other words, the above results collectively establish that **TA8** predominantly mediates exchange of Cl^- and OH^- anions across the membrane.

The chloride-transport behaviour by **TA8** was then examined in the planar lipid bilayer. The evolved single channel current traces for chloride at various voltages (Fig. 2f) conclusively demonstrate that **TA8**-mediated chloride transport occurs through a channel, rather than a carrier, mechanism. Fitting of a linear current–voltage (*I–V*) curve yields a Cl^- conductance (γ_{Cl^-}) of 396.5 ± 10.3 fS for **TA8**.

In our effort to elucidate the anion selectivity of **TA8** using the LUV scheme shown in Fig. 3a, we were surprised to find that both I^- and ClO_4^- are transported much faster than Cl^- at the same concentration of 20 μM after subtracting background signals and further normalization (Fig. 3b). These findings prompted us to carry out a more systematic examination of anion transport involving all five types of anions by the remaining four **TA** channels. Our summative results in Fig. 3b show that, except for the chloride anions for which **TA8** acts as the best channel, **TA12** induces the fastest transports for all other four anions (Br^-, I^-, ClO_4^- and NO_3^-), while **TA14** displays very high selectivity toward I^- anions relative to both Br^- and Cl^- anions. In comparison, fractional ion transport activities of Cl^-, I^- or ClO_4^- were measured to be 3.5, 6.1 and 10.0% for **TA4**, suggesting that highly active transport of I^- or ClO_4^- by **TA12** is mediated by a channel, rather than a carrier, mechanism, which is also consistent with single channel current traces obtained for chloride transport by **TA8** (Fig. 2f).

On the basis of initial rate constants (Fig. 3c and Fig. S2, ESI†), I^- anions are transported by **TA12** at a speed that is about 20 and 41 times those for Br^- and Cl^- anions, respectively. Following the Hill analysis, the EC_{50} values at which channels achieve 50% ion transport activity were determined to be 3.0 and 12.1 μM for ClO_4^- (Fig. 3d) and I^- (Fig. S3, ESI†) anions, respectively. On this basis, **TA12**-mediated transport of ClO_4^-

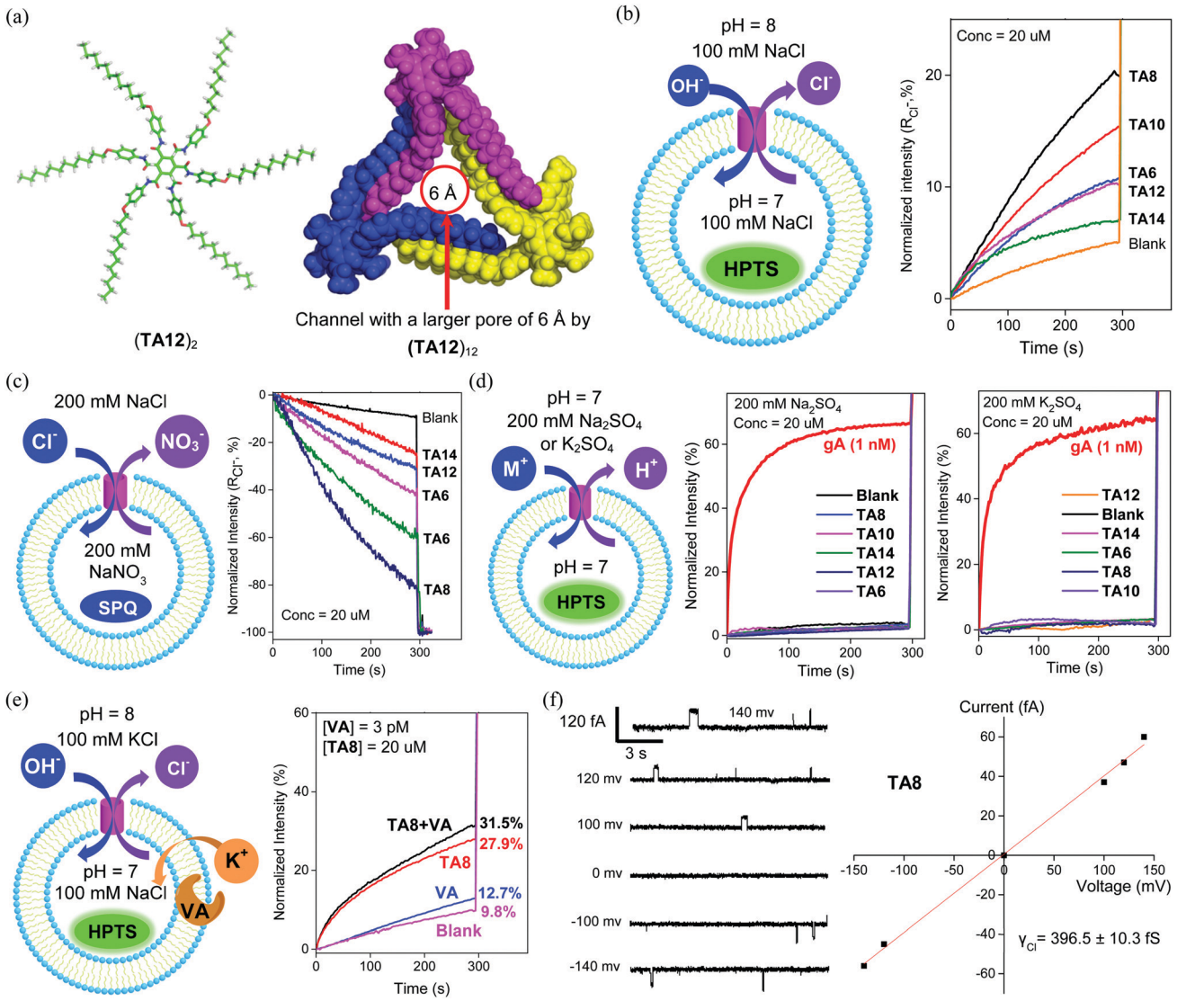

Fig. 2 (a) A schematic illustration of **TA12**, forming a larger pore of 6 Å obtained using PM6D3. (b) pH-sensitive HPTS assay for evaluating and comparing the ion transport activities of ion channels; $R_{Cl^-} = (I_{Cl^-} - I_0)/(I_{Triton} - I_0)$ whereas I_{Cl^-} and I_0 are the ratiometric values of I_{460}/I_{403} at t = 300 s before addition of Triton, and I_{Triton} is the ratiometric value of I_{460}/I_{403} at t = 300 s right after addition of Triton. (c) Chloride-sensitive SPQ assay for evaluating chloride-transport functions. (d) Sulphate-containing LUV assay for assessing the applicability of Na^+-based ion exchange as the ion transport mechanism. (e) Valinomycin-based LUV assay for comparing relative transport rates between OH^- and Cl^-. (f) Single channel current traces for chloride transport recorded at various voltages in symmetric baths (*cis* chamber = *trans* chamber = 1 M KCl) as well as the determined chloride conductance value for **TA8**.

anions is four times as fast as that of I^- anions. It might be worth pointing out that the initial rate constants for I^- transport decrease much more rapidly upon decreasing the channel concentration than those for ClO_4^- transport (Fig. S4 *vs.* S5, ESI†).

Lastly, with respect to a typical thickness of 34 Å for the hydrophobic membrane region, an inter-planar separation distance of 3.69 Å observed for **TA4** in the crystal structure (Fig. 1b)[7b] suggests that 10 molecules of **TA12** would be required to form a rod-like structure that can fully span the hydrophobic membrane region. In this regard, the EC_{50} value in terms of the effective channel concentration for ClO_4^- is 0.3 μM. This value corresponds to a channel : lipid molar ratio of 1 : 104 or 0.96 mol%, certainly pointing to a highly efficient transport of ClO_4^- anions by **TA12**.

To summarize, stimulated by the sizable channels/voids created *via* a hexagonal arrangement of 1D rod-like structures that were assembled from **TA4** molecules, we have successfully uncovered a new class of synthetic anion channels with unusual selectivities. Based on the EC_{50} values, the most active and highly selective anion channel **TA12** transports ClO_4^- anions three times faster than I^- anions, which, on the basis of the initial rate constants, are transported drastically much faster than Br^- and Cl^- anions by 19 and 40 times, respectively. Further exquisite optimization of the peripheral substituents may lead to improved activities with interesting anion selectivities.

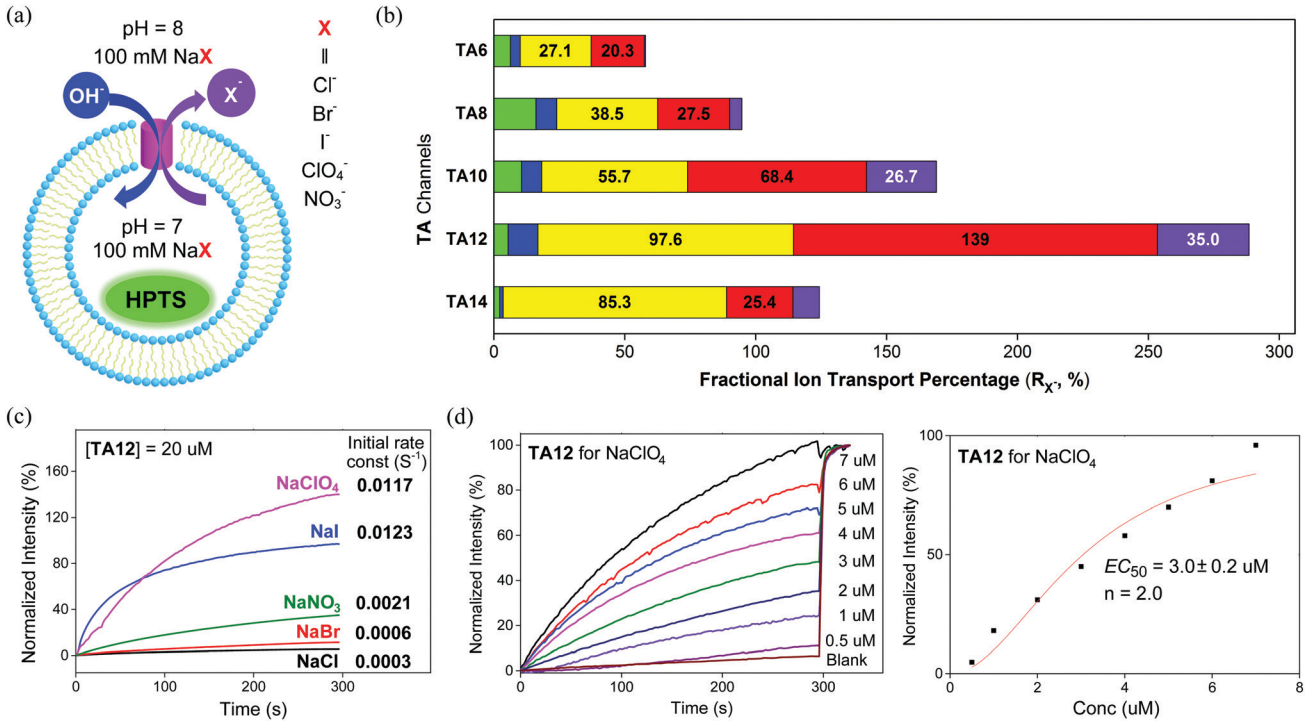

Fig. 3 (a) LUV scheme for determining anion selectivity. (b) Fractional transport activities measured for five types of anions by all five **TA** channels. (c) Initial rate constants determined for **TA12**-mediated anion transport. (d) Determination of the EC_{50} value for **TA12**-mediated transport of ClO_4^- using the Hill analysis.

This work is funded by the Institute of Bioengineering and Nanotechnology (Biomedical Research Council, Agency for Science, Technology and Research, Singapore), the Natural Science Foundation of Hunan Province of China (2018JJ3193) and the construct program of applied characteristic discipline in Hunan University of Science and Engineering.

Conflicts of interest

There are no conflicts to declare.

Notes and references

1 I. Tabushi, Y. Kuroda and K. Yokota, *Tetrahedron Lett.*, 1982, **23**, 4601.
2 (*a*) J. T. Davis, O. Okunola and R. Quesada, *Chem. Soc. Rev.*, 2010, **39**, 3843; (*b*) P. R. Brotherhood and A. P. Davis, *Chem. Soc. Rev.*, 2010, **39**, 3633; (*c*) S. Matile, A. Vargas Jentzsch, J. Montenegro and A. Fin, *Chem. Soc. Rev.*, 2011, **40**, 2453; (*d*) J. Montenegro, M. R. Ghadiri and J. R. Granja, *Acc. Chem. Res.*, 2013, **46**, 2955; (*e*) T. M. Fyles, *Acc. Chem. Res.*, 2013, **46**, 2847; (*f*) F. Otis, M. Auger and N. Voyer, *Acc. Chem. Res.*, 2013, **46**, 2934; (*g*) G. W. Gokel and S. Negin, *Acc. Chem. Res.*, 2013, **46**, 2824; (*h*) F. De Riccardis, I. Izzo, D. Montesarchio and P. Tecilla, *Acc. Chem. Res.*, 2013, **46**, 2781; (*i*) L. D. Mosgaard and T. Heimburg, *Acc. Chem. Res.*, 2013, **46**, 2966; (*j*) B. Gong and Z. Shao, *Acc. Chem. Res.*, 2013, **46**, 2856; (*k*) D. S. Kim and J. L. Sessler, *Chem. Soc. Rev.*, 2015, **44**, 532; (*l*) J.-Y. Chen and J.-L. Hou, *Org. Chem. Front.*, 2018, **5**, 1728.
3 (*a*) A. Vargas Jentzsch and S. Matile, *J. Am. Chem. Soc.*, 2013, **135**, 5302; (*b*) A. Gilles and M. Barboiu, *J. Am. Chem. Soc.*, 2016, **138**, 426; (*c*) C. L. Ren, J. Shen and H. Q. Zeng, *J. Am. Chem. Soc.*, 2017, **139**, 12338; (*d*) C. Ren, X. Ding, A. Roy, J. Shen, S. Zhou, F. Chen, S. F. Yau Li, H. Ren, Y. Y. Yang and H. Zeng, *Chem. Sci.*, 2018, **9**, 4044.
4 (*a*) Y. Lai and R. L. Gallo, *Trends Immunol.*, 2009, **30**, 131; (*b*) R. E. W. Hancock, E. F. Haney and E. E. Gill, *Nat. Rev. Immunol.*, 2016, **16**, 321; (*c*) S. M. Mandal, S. Sharma, A. K. Pinnaka, A. Kumari and S. Korpole, *BMC Microbiol.*, 2013, **13**, 152; (*d*) F. S. Tareq, M. A. Lee, H.-S. Lee, Y.-J. Lee, J. S. Lee, C. M. Hasan, M. T. Islam and H. J. Shin, *Org. Lett.*, 2014, **16**, 928; (*e*) A. Makovitzki, D. Avrahami and Y. Shai, *Proc. Natl. Acad. Sci. U. S. A.*, 2006, **103**, 15997; (*f*) G. Wiedman, S. Y. Kim, E. Zapata-Mercado, W. C. Wimley and K. Hristova, *J. Am. Chem. Soc.*, 2017, **139**, 937; (*g*) A. J. Krauson, O. M. Hall, T. Fuselier, C. G. Starr, W. B. Kauffman and W. C. Wimley, *J. Am. Chem. Soc.*, 2015, **137**, 16144; (*h*) R. Rathinakumar and W. C. Wimley, *J. Am. Chem. Soc.*, 2008, **130**, 9849; (*i*) Z. Y. Ong, N. Wiradharma and Y. Y. Yang, *Adv. Drug Delivery Rev.*, 2014, **78**, 28.
5 (*a*) E. Wolf, P. S. Kim and B. Berger, *Protein Sci.*, 1997, **6**, 1179; (*b*) S. Y. Lau, A. K. Taneja and R. S. Hodges, *J. Biol. Chem.*, 1984, **259**, 13253; (*c*) T. Sasaki and E. T. Kaiser, *J. Am. Chem. Soc.*, 1989, **111**, 380; (*d*) C. P. Hill, D. H. Anderson, L. Wesson, W. F. DeGrado and D. Eisenberg, *Science*, 1990, **249**, 543; (*e*) C. E. Schafmeister, S. L. LaPorte, L. J. W. Miercke and R. M. Stroud, *Nat. Struct. Biol.*, 1997, **4**, 1039; (*f*) R. E. Hibbs and E. Gouaux, *Nature*, 2011, **474**, 54; (*g*) X. Hou, L. Pedi, M. M. Diver and S. B. Long, *Science*, 2012, **338**, 1308; (*h*) M. D. Peraro and F. G. van der Goot, *Nat. Rev. Microbiol.*, 2015, **14**, 77.
6 C. L. Ren, F. Zeng, J. Shen, F. Chen, A. Roy, S. Y. Zhou, H. S. Ren and H. Q. Zeng, *J. Am. Chem. Soc.*, 2018, **140**, 8817.
7 (*a*) M. P. Lightfoot, F. S. Mair, R. G. Pritchard and J. E. Warren, *Chem. Commun.*, 1999, 1945; (*b*) V. Nagarajan and V. R. Pedireddi, *Cryst. Growth Des.*, 2014, **14**, 1895; (*c*) S. Hasegawa, S. Horike, R. Matsuda, S. Furukawa, K. Mochizuki, Y. Kinoshita and S. Kitagawa, *J. Am. Chem. Soc.*, 2007, **129**, 2607; (*d*) S. Cantekin, T. F. A. de Greef and A. R. A. Palmans, *Chem. Soc. Rev.*, 2012, **41**, 6125.

